FEBS Letters 582 (2008) 3230–3236

Cholesterol displacement by ceramide in sphingomyelin-containing liquid-ordered domains, and generation of gel regions in giant lipidic vesicles

Jesús Sot, Maitane Ibarguren, Jon V. Busto, L.-Ruth Montes, Félix M. Goñi, Alicia Alonso*

Unidad de Biofísica (Centro Mixto CSIC-UPV/EHU), and Departamento de Bioquímica, Universidad del País Vasco, P.O. Box 644, 48080 Bilbao, Spain

Received 7 August 2008; revised 12 August 2008; accepted 15 August 2008

Available online 26 August 2008

Edited by Sandro Sonnino

Abstract Fluorescence confocal microscopy and differential scanning calorimetry are used in combination to study the phase behaviour of bilayers composed of PC:PE:SM:Chol equimolecular mixtures, in the presence or absence of 10 mol% egg ceramide. In the absence of ceramide, separate liquid-ordered and liquid-disordered domains are observed in giant unilamellar vesicles. In the presence of ceramide, gel-like domains appear within the liquid-ordered regions. The melting properties of these gel-like domains resemble those of SM:ceramide binary mixtures, suggesting Chol displacement by ceramide from SM:Chol-rich liquid-ordered regions. Thus three kinds of domains coexist within a single vesicle in the presence of ceramide: gel, liquid-ordered, and liquid-disordered. In contrast, when 10 mol% egg diacylglycerol is added instead of ceramide, homogeneous vesicles, consisting only of liquid-disordered bilayers, are observed.

Keywords: Cholesterol; Ceramide; Sphingomyelin; Membrane domains; Fluorescence confocal microscopy; Differential scanning calorimetry

1. Introduction

The last decade has witnessed an outburst of research activity concerning the significance of lateral heterogeneity, i.e. existence of domains, in cell membranes. Once denied, then fiercely debated, it is now generally accepted that biomembranes are compositionally and functionally heterogeneous along their surface [1]. Studies in pure lipid vesicles (liposomes) have demonstrated that, even with simple two-lipid mixtures, domain formation can occur. The coexistence of gel and fluid [2,3], gel and liquid-ordered [4] and that of liquid-ordered and liquid-disordered domains [5] has been shown by a variety of physical methods (see reviews by Edidin [6] and Simons and Vaz [7]). The advent of giant unilamellar vesicles (GUV) [8,9] and the application of confocal fluorescence microscopy [10] has allowed visualization of domains and domain coexistence in a variety of lipid membranes. In particular, observation of three-domain coexistence in single vesicles has been achieved, either in POPC:Cer:Chol mixtures [11], or in DPPC:DOPC:Chol mixtures [12]. Chiantia et al. [13] observed coexistence of three kinds of domains in SM:PC:Chol:Cer supported bilayers.

Among membrane domains, those enriched in ceramide have received particular attention because Cer formation is one of the early steps in the apoptotic pathway [14,15] (see review by Taha et al. [16]). Ceramide is hardly miscible with other membrane lipids, thus it tends to segregate laterally into gel-like Cer-enriched domains [17] (see reviews in [18,19]). London and co-workers [20,21] have made the interesting observation that Cer displaces Chol from ordered lipid domains containing phosphatidylcholines, or SM, and Chol. This has been confirmed by other investigators [13,22,23]. The phenomenon is probably related to the previous observation of cholesterol displacement from plasma membranes induced by sphingomyelinase activity [24,25].

In the present study, we have applied confocal fluorescence microscopy to the study of GUV's composed of PC:PE:SM:Chol (1:1:1:1, mole ratio), a lipid mixture used by us in previous studies with the aim of mimicking the complex cell plasma membranes [26,27]. The images reveal that in these vesicles, liquid-ordered and liquid-disordered phase separation occurs. Moreover, addition of Cer gives rise to gel-like domains, that exhibit cooperative melting by differential scanning calorimetry, while addition of the structurally similar diacylglycerol blurs all interdomain boundaries.

2. Materials and methods

2.1. Materials

Egg phosphatidylcholine (PC), egg phosphatidylethanolamine (PE) and egg diacylglycerol (DAG) were purchased from Lipid Products (South Nutfield, UK). Egg SM, egg Cer and Chol were from Avanti Polar Lipids (Alabaster, AL). 1,1′-Dioctadecyl-3,3,3′3′-tetramethylindocarbocyanine perchlorate (DiI) and Alexa Fluor 488 C_5-maleimide were from Invitrogen (Eugene, OR). NBD-Cer was a kind gift of Dr. G. Fabrias (IIQAB, CSIC, Barcelona, Spain).

2.2. GUV preparation and fluorescence microscopy

GUVs were prepared using the electroformation method developed by Angelova et al. [8]. For GUV observation at room temperature, a chamber supplied by L.A. Bagatolli (Odense, Denmark) was used, that allows direct GUV visualization under the microscope [11]. A PRET-GUV 4 Chamber supplied by Industrias Técnicas ITC (Bilbao, Spain) was used for vesicle preparation when observation of GUVs at 37 °C or 43 °C was required. Stock solutions of lipids (0.2 mg/ml total lipid containing either 0.2 mol% DiI or 0.2 mol% DiI and 0.4 mol% NBD-Cer) were prepared in a chloroform:methanol (9:1, v/v) solution. Three microlitres of the appropriate lipid stocks were added on the surface of

*Corresponding author. Fax: +34 94 601 33 60.
E-mail address: alicia.alonso@ehu.es (A. Alonso).

0014-5793/$34.00
doi:10.1016/j.febslet.2008.08.016

Pt electrodes and solvent traces were removed by evacuating the chamber under high vacuum for at least 2 h.

2.2.1. Direct visualization of GUVs at room temperature

The Pt electrodes were covered with 400 μl of 10 mM HEPES, pH 7.4 previously heated at 60 °C. When required, 3 μM Alexa Fluor 488 was added to the HEPES Buffer. The Pt wires were connected to an electric wave generator (TG330 function generator, Thurlby Thandar Instruments, Huntington, UK) under AC field conditions (10 Hz, 1 V) for 2 h at 60 °C. In some cases, in order to obtain a more clear domain separation, after 2 h incubation at 60 °C heating was switched off, while the generator was switched off only when the temperature of the chamber reached 37 °C. When Alexa 488 was added, the excess dye was removed by washing the chamber 7 times with 10 mM HEPES, pH 7.4.

2.2.2. Observation of GUVs at 37 °C or 43 °C

The Pt electrodes were covered with 400 μl of 200 mM sucrose, previously heated at 60 °C. The Pt electrodes were connected to a generator (TG330 function generator, Thurlby Thandar Instruments) under AC field conditions (10 Hz, 1 V for 2 h, followed by 1 Hz, 1 V, 10 min) at 60 °C. Finally, the AC field was turned off and the vesicles (in 200 mM Sucrose) were collected from the PRETGUV 4 chamber with a pipette and transferred to a Micro-Incubator Platform DH-40i supplied by Warner Instruments (Hamden, USA) containing an equiosmolar buffer solution 95 mM NaCl, 10 mM HEPES, pH 7.4. Due to the different density between the two solutions the vesicles sedimented at the bottom of the chamber, which facilitated observation under the microscope.

After GUV formation, the chambers were located in an inverted confocal fluorescence microscope (Nikon D-ECLIPSE C1, Nikon Inc., Melville, NY). The excitation wavelengths were 430 nm for NBD-Cer, 488 nm for Alexa 488 and 561 nm for DiI. The images were collected through two different channels using band-pass filters of 515 ± 15 nm for the NBD-Cer and Alexa 488, and 593 ± 20 nm for the DiI. Image treatment and quantification was performed using the software EZ-C1 3.20 (Nikon Inc.). No difference in domain size, formation or distribution was observed in the GUVs along the observation period or after laser exposure.

2.3. Multilamellar vesicle preparation

For multilamellar (MLV) liposome preparation the lipids were dissolved in chloroform/methanol (2:1) and mixed as required, and the solvent was evaporated to dryness under a stream of nitrogen. Traces of the solvent were removed by evacuating the samples under high vacuum for at least 2 h. The samples were hydrated at 45 °C in 20 mM PIPES, 150 mM NaCl, 1 mM EDTA, pH 7.4, helping dispersion by stirring with a glass rod. The final lipid concentration was measured as lipid phosphorus.

2.4. Differential scanning calorimetry

For differential scanning calorimetry MLV were used. Both lipid suspension and buffer were degassed before being loaded into the sample or reference cell of a VP-DSC Microcalorimeter (MicroCal, Northampton, MA). The final concentration of PC:PE:SM:Chol (1:1:1:1, mole ratio) was 10 mM. Four heating scans, and occasionally a cooling one, at 45 °C/h were recorded for each sample. After the first one, successive heating scans on the same sample gave always superimposable thermograms. Transition temperatures, enthalpies, and widths at half-height were determined using the software ORIGIN (MicroCal) provided with the calorimeter.

3. Results and discussion

3.1. Vesicle morphology

GUV's composed of PC:SM:PE:Chol (1:1:1:1, mole ratio), prepared by electroformation, and stained with fluorescent probes were examined by confocal fluorescence microscopy (Fig. 1). At room temperature (columns A and B) the vesicles present low mobility, and different planes of the same vesicle can be micrographed, so that three-dimensional reconstruction is readily achieved. PC:SM:PE:Chol vesicles display lateral lipid heterogeneity, i.e. distinct lipid domains are seen. Vesicles in column A have been stained with DiI, which has a preference for the more fluid and disordered phases [28]. When vesicle preparation includes Alexa 488, a water-soluble stain that remains partly entrapped in the vesicles [9] (Fig. 1, column B), other domains become visible. Under our conditions, most vesicles appear to contain two domains, the more disordered one being larger in size (Fig. 1 and Supplementary Material Fig. S1). At 37 °C, the vesicles are not stuck to the coverglass as in the case of the direct visualization protocol when the

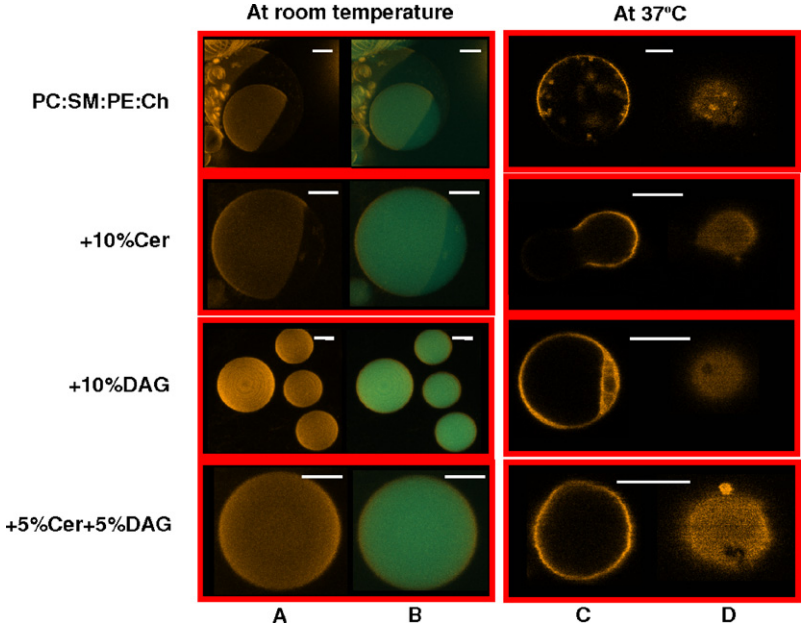

Fig. 1. Confocal microscopy of representative GUVs. Composition is given in the left-hand column. (A, B) Three-dimensional reconstructions at room temperature; (C, D) respectively, equatorial and polar planes at 37 °C. (A, C, D) DiI stain; (B) DiI + Alexa 488 stain. Bar = 10 μm.

vesicles are stuck to the Pt electrodes. For this reason the vesicles can diffuse along the coverglass. So adding the second fluorescent stain is impracticable because the washing step causes the vesicles to wash off the coverglass. Images at 37 °C (Fig. 1, columns C and D) are only stained with DiI, and only two planes: equatorial (column C) and polar (column D) are shown. Still the situation at 37 °C appears to be very similar to that at room temperature, with vesicles composed of one, larger and brighter, and one, smaller and dimmer, domains.

GUV containing either additional 10 mol% Cer, or additional 10 mol% DAG or additional 5 mol% Cer + 5 mol% DAG, were formed and examined by confocal microscopy as above. Typical images are also shown in Fig. 1 and in Supplementary Material Fig. S1. Additional 10 mol% Cer does not cause significant changes in the morphology at room temperature (although domain structure is not the same as in the absence of Cer, see below) while at 37 °C peanut-shaped vesicles are observed. The tendency towards bleb formation is probably due to the molecular geometry of ceramide [18,29–31]. Narrow "waists" separating darker from brighter domains can be seen more clearly at room temperature in vesicles containing ceramide and formed using a slightly different protocol as above (Fig. 2). These peanut-shaped vesicles are only detected in the presence of ceramide. Additional 10 mol% DAG, on the contrary, gives rise to spherical vesicles at all temperatures, and suppresses lateral heterogeneity, i.e. no domain separation is seen, rather the whole vesicles appear uniformly stained by DiI (Fig. 1). Interestingly (column C) some DAG-containing vesicles appear to contain remnants of fusion events, as observed by cryo-TEM on a comparable system [32]. Finally, the equimolar mixture DAG + Cer also gives rise to homogeneous vesicles, although in some cases, as in the polar domain of the vesicles photographed at 37 °C (Fig. 1, column D) a small, presumably Cer-enriched, dark domain is observed [28].

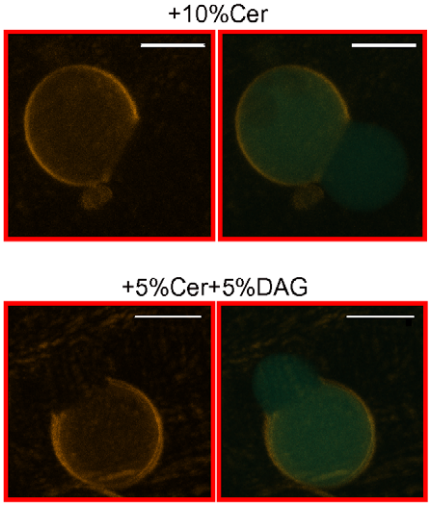

Fig. 2. Confocal microscopy of representative GUV's. In this case, in the course of GUV preparation, the bath, originally at 60 °C, was switched off to allow cooling down of the system, while the electric wave generator was kept on. Vesicle composition is: (top) SM:PC:PE:Chol (1:1:1:1, mole ratio) + 10 mol% Cer; (bottom) PC:PE:SM:Chol (1:1:1:1, mole ratio) + 5 mol% DAG + 5 mol% DAG. Fluorescence stain: DiI (left-hand side); DiI + Alexa 488 (right-hand side). Bar = 10 μm.

3.2. Differential scanning calorimetry and the nature of lipid domains

Multilamellar vesicles (MLV) of the same composition as the GUV described in Fig. 1 were examined by differential scanning calorimetry (DSC). MLV are more convenient than GUV for the calorimetric studies, and abundant data in the literature support the idea that phase behaviour should be very similar in both membrane models (see, e.g. [33,34]). MLV composed of PC:SM:PE:Chol at equimolar ratios did not give rise to any endotherm in the 10–60 °C range (Fig. 3). Only one of these lipids, SM, when in the pure state, exhibits a gel-fluid transition in this temperature range [35,36], but in binary mixtures with cholesterol the transition is abolished as a liquid-ordered phase forms. Liquid-ordered phases do not exhibit endotherms in the temperature range of our studies (10–60 °C) [37,38]. The DSC and microscopy data for the PC:SM:PE:Chol mixtures are thus compatible with the coexistence of a liquid-ordered and a fluid-disordered phase.

The situation is quite different when additional 10 mol% Cer is incorporated into the vesicle composition (Fig. 3) since a wide but clearly visible endotherm is detected (midpoint transition temperature $T_m = 35.5 \pm 0.11$ °C; width at half-height WHH = 8.6 ± 0.45 °C; enthalpy change $\Delta H = 1.1 \pm 0.05$ kcal/mol). The simplest interpretation of the data in Figs. 1–3 is that Cer is displacing Chol [20] and giving rise to gel-like, SM- and Cer-enriched domains, which melt down in the 20–45 °C temperature range. This is in agreement with previously published DSC on the melting data of SM:Cer mixtures [28].

DAG does not give rise to high-melting domains with any of the other four lipids, thus no endotherm is observed with MLV composed of PC:SM:PE:Chol:DAG (1:1:1:1:0.4, mole ratio) (Fig. 3). This is accompanied by the lack of lateral heterogeneity in the GUV (Fig. 1 and Supplementary Material Fig. S1). The uniformly bright DiI staining of the DAG-containing vesicles and lack of DSC endotherm suggest that their bilayers are in the liquid-disordered state. Finally, the mixture containing additional 5 mol% of both Cer and DAG represents an inter-

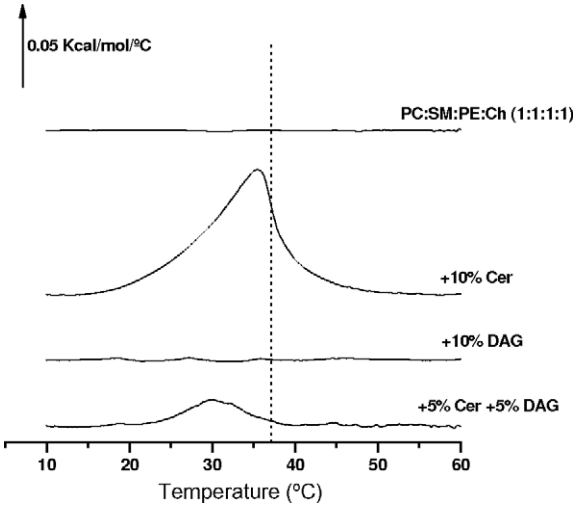

Fig. 3. Differential scanning calorimetry of the lipid mixtures under study. Lipids were dispersed in the form of MLV. Third heating scans. Lipid composition is given at the right-hand side of each thermogram. Thermodynamic parameters are given in the main text.

mediate case, with a smaller endotherm (Fig. 3) (midpoint transition temperature $T_m = 29.0 \pm 0.84$ °C; width at half-height WHH = 8.7 ± 0.91 °C; enthalpy change $\Delta H = 0.16 \pm 0.009$ kcal/mol) and correspondingly smaller and/or more scarce rigid domains (Fig. 1 and Supplementary Material Fig. S1).

In principle, the different effects of DAG and Cer could be due to either the difference in polar headgroups, or the difference in chain length/unsaturation. Without denying the possible influence of the headgroups, our own (unpublished) experiments point to the different degrees of alkyl chain unsaturation as one major cause for the different behaviour of DAG and Cer towards formation of high-T melting domains. The egg ceramide used in the present study contains >80% saturated N-acyl chains, and its gel-fluid transition under full hydration conditions is at ca. 90 °C [19], while egg DAG contains only ca. 40% saturated acyl chains and its gel-fluid transition occurs below 0 °C. In binary mixtures with egg SM, the disaturated dipalmitoylglycerol (DPG) gave rise to high-T melting domains virtually under the same conditions as egg Cer (Fig. 4). Note however that other experimental data underline certain differences between glycerolipids and sphingolipids that appear to be due to the headgroups, rather than to the alkyl chains [39,40].

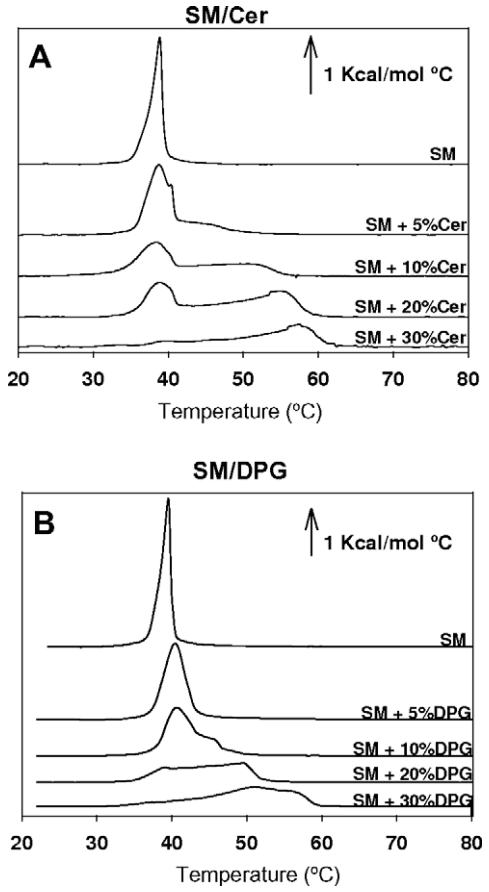

Fig. 4. Differential scanning calorimetry of SM/Cer and SM/dipalmitoylglycerol mixtures. Lipids were dispersed in the form of MLV. Third heating scans. Lipid composition (in mol%) is given at the right-hand side of the corresponding thermogram. (A) SM/Cer mixtures; (B) SM/DPG mixtures.

3.3. Three-domain coexistence

The next question deals with the localisation of the Cer-rich domains giving rise to the endotherms seen in Fig. 3. According to London's hypothesis [20] of the displacement of Chol by Cer in mixtures with SM, Cer-rich domains should appear either near or within the liquid-ordered regions revealed by DiI/Alexa 488 in Fig. 1. This was shown to be the case by a series of observations in which a third fluorescent probe, namely NBD-Cer was used. This probe consists of a ceramide in which the N-acyl chain has been derivatised with the fluorescent NBD. In a somewhat counterintuitive way, NBD-Cer is *excluded* from the gel-like Cer-rich domains, presumably because the NBD moiety prevents the tight packing of N-acyl chains that occurs in the gel-like Cer-rich domains [28,29,41]. This is shown in Supplementary Material Fig. S2, in which egg PC/egg Cer (80:20, mole ratio) GUV were examined. In this mixture, gel Cer-enriched domains coexist with fluid PC-enriched ones [29]. Both DiI and NBD-Cer are excluded from the gel domains. The gel-like nature of Cer-containing domains is reinforced by the observation that, in 3D images, the boundaries of these domains are not perfectly circular, as would happen for coexisting fluid domains. The presence of fluorescent probes in the systems, under our conditions, did not cause changes in the DSC behaviour of the samples under study (data not shown).

In the quaternary mixture PC:PE:SM:Chol (1:1:1:1, mole ratio) NBD-Cer is seen to distribute uniformly among the liquid-ordered and liquid-disordered domains (Fig. 5). Thus, NBD-Cer allows the distinction between liquid-ordered and gel domains. Interestingly, when PC:PE:SM:Chol GUV's are heated up to 43 °C the DiI distribution reveals that the dark domains remain present, as expected from liquid-ordered phases (Fig. 5, bottom pictures). NBD-Cer at 43 °C is partially photobleached, thus the GUV image is dimmer than at room temperature, although it undoubtedly reveals uniform distribution of the probe along the whole vesicle diameter.

In vesicles containing 10 mol% Cer, i.e. the conditions under which DSC reveals gel-fluid transitions (Fig. 3), NBD-Cer shows gel domains as small regions within larger liquid-ordered domains (Fig. 6, top). No such gel domains were seen in the absence of Cer (Fig. 5). Moreover, upon heating at 43 °C, i.e. the upper end of the calorimetric gel-fluid transition in Fig. 3, the gel domains are no longer detected, while the liquid-ordered domains remain intact (Fig. 6, bottom). In order to investigate the minimum concentration of ceramide that gives rise to visible gel domains in GUV, vesicles were examined that contained 7.5, 5.0, and 2.5 mol% ceramide, respectively, under the same conditions as in the experiment in Fig. 6. Gel domains were clearly seen with 7.5 mol% ceramide (Supplementary Material Fig. S3), while with 5.0 mol% the difference between gel and liquid-ordered domains become fuzzy. Finally, with 2.5 mol% ceramide, no gel domain could be detected (Supplementary Material Fig. S3). This is in agreement with DSC data of various ceramide/phospholipid mixtures, according to which detection of lateral separation of Cer-enriched domains requires at least 3–5 mol% ceramide [19,29].

The driving force for sterol displacement by ceramide would be the hydrophobic effect that tends to minimise unfavourable contact between the hydrocarbon groups of the small headgroup lipids (ceramides and sterols) and the surrounding aqueous environment [22,23]. Hydrocarbon–water contact would be prevented in ordered domains because of the capacity of

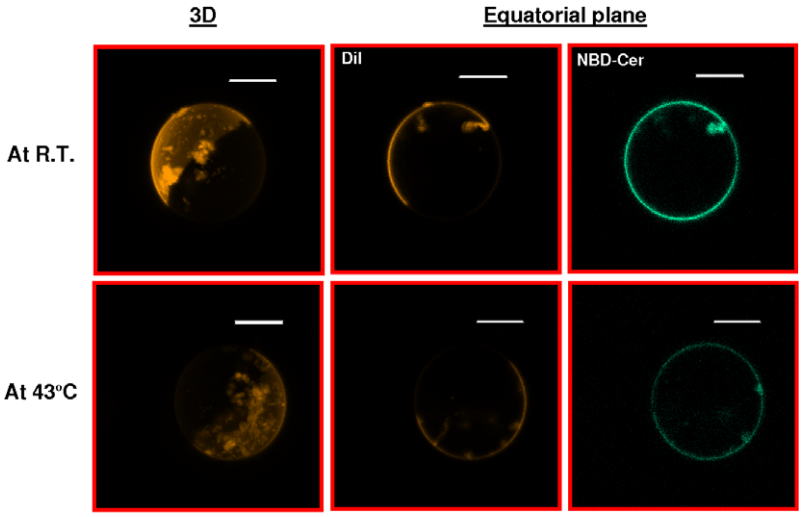

Fig. 5. Uniform distribution of NBD-Cer in liquid-ordered and fluid-disordered domains. Confocal microscopy of representative GUV's. Composition PC:PE:SM:Chol (1:1:1:1, mole ratio) as Fig. 1. (top) Pictures taken at room temperature; (bottom) pictures taken at 43 °C. Stain: DiI (left-hand side) or NBD-Cer (right-hand side). Bar = 10 μm.

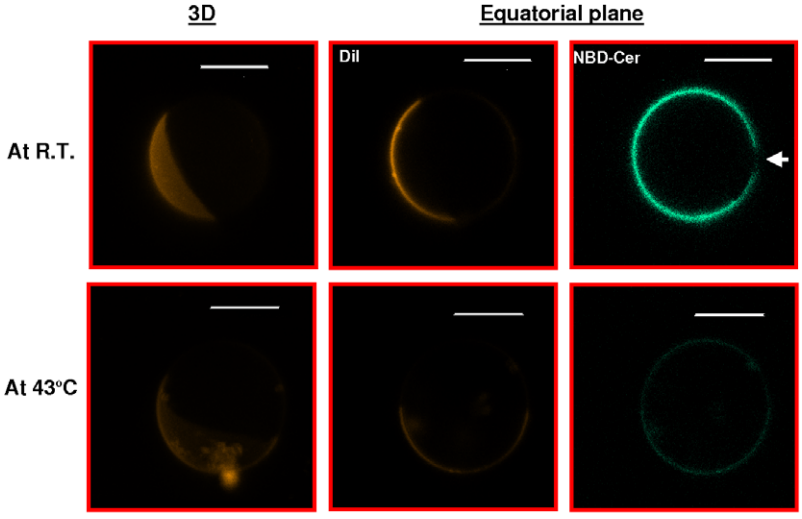

Fig. 6. Generation of gel-like domains in the presence of Cer. Confocal microscopy of representative GUV's. Composition PC:PE:SM:Chol (1:1:1:1, mole ratio) + 10 mol% Cer. (A, B) Room temperature, 3D-reconstruction; (C, D) room temperature, equatorial planes; (E, F) the same vesicles as in (C, D), but at 43 °C, equatorial planes. Stain: DiI (left-hand side) or NBD-Cer (right-hand side). The white arrows point to gel-like domains, from which NBD-Cer is excluded. Bar = 10 μm.

certain lipids with large headgroups (sphingomyelin and phosphatidylcholines) to accommodate small headgroup lipids in the ordered domain lattice. Ceramide would replace sterols with advantage from this point of view. See in this respect the "molecular cavity" concept developed for ganglioside/ceramide mixtures by Carrer and Maggio [42]. The same phenomenon would occur when SM is degraded by a sphingomyelinase to Cer, in bilayers in the presence of Chol [41,43], even if Cer generated in situ by a sphingomyelinase does not segregate laterally in exactly the same way as premixed Cer, clusters of Cer-rich domains being observed in the former case [41]. Note that, strictly speaking, neither in this or in related studies is there a direct demonstration of Chol displacement by Cer, since quantitative analysis of the different domains has not been performed yet. However, the simplest hypothesis that explains the properties of the newly formed gel domains is still that of Cer-rich, Chol-poor membrane regions.

In conclusion, we have produced morphological evidence that addition of Cer to vesicles containing PC:PE:SM:Chol leads very likely to partial replacement of Chol by Cer in the SM:Chol-rich liquid-ordered domains, with formation of smaller SM:Cer-rich gel domains. This would be in agreement with previous predictions and observations [13,20,21], and constitutes an unusual example of three-phase coexistence with in a single vesicle.

Acknowledgements: The authors are indebted to Dr. G. Fabrias for her gift of NBD-Cer. This work was supported in part by Grants from Spanish Ministerio de Educación y Ciencia (BFU 2005-06095) (A.A.), (MEC07-62062) (F.M.G.), and the Basque Government (IT461-07) (F.M.G.). M.I. was a graduate student supported by the Basque government.

Appendix A. Supplementary material

Supplementary data associated with this article can be found, in the online version, at doi:10.1016/j.febslet.2008.08.016.

References

[1] Mukherjee, S. and Maxfield, F.R. (2004) Membrane domains. Annu. Rev. Cell Dev. Biol. 20, 839–866.

[2] Almeida, P.F., Vaz, W.L. and Thompson, T.E. (1993) Percolation and diffusion in three-component lipid bilayers: effect of cholesterol on an equimolar mixture of two phosphatidylcholines. Biophys. J. 64, 399–412.

[3] Bar, L.K., Barenholz, Y. and Thompson, T.E. (1997) Effect of sphingomyelin composition on the phase structure of phosphatidylcholine–sphingomyelin bilayers. Biochemistry 36, 2507–2516.

[4] Veiga, M.P., Arrondo, J.L., Goñi, F.M., Alonso, A. and Marsh, D. (2001) Interaction of cholesterol with sphingomyelin in mixed membranes containing phosphatidylcholine, studied by spin-label ESR and IR spectroscopies. A possible stabilization of gel-phase sphingolipid domains by cholesterol. Biochemistry 40, 2614–2622.

[5] Collado, M.I., Goñi, F.M., Alonso, A. and Marsh, D. (2005) Domain formation in sphingomyelin/cholesterol mixed membranes studied by spin-label electron spin resonance spectroscopy. Biochemistry 44, 4911–4918.

[6] Edidin, M. (2003) The state of lipid rafts: from model membranes to cells. Annu. Rev. Biophys. Biomol. Struct. 32, 257–283.

[7] Simons, K. and Vaz, W.L. (2004) Model systems, lipid rafts, and cell membranes. Annu. Rev. Biophys. Biomol. Struct. 33, 269–295.

[8] Angelova, M.I. and Tsoneva, I. (1999) Interactions of DNA with giant liposomes. Chem. Phys. Lipids 101, 123–137.

[9] Montes, L.R., Alonso, A., Goñi, F.M. and Bagatolli, L.A. (2007) Giant unilamellar vesicles electroformed from native membranes and organic lipid mixtures under physiological conditions. Biophys. J. 93, 3548–3554.

[10] Bagatolli, L.A. (2003) Direct observation of lipid domains in free standing bilayers: from simple to complex lipid mixtures. Chem. Phys. Lipids 122, 137–145.

[11] Fidorra, M., Duelund, L., Leidy, C., Simonsen, A.C. and Bagatolli, L.A. (2006) Absence of fluid-ordered/fluid-disordered phase coexistence in ceramide/POPC mixtures containing cholesterol. Biophys. J. 90, 4437–4451.

[12] de Almeida, R.F., Borst, J., Fedorov, A., Prieto, M. and Visser, A.J. (2007) Complexity of lipid domains and rafts in giant unilamellar vesicles revealed by combining imaging and microscopic and macroscopic time-resolved fluorescence. Biophys. J. 93, 539–553.

[13] Chiantia, S., Kahya, N., Ries, J. and Schwille, P. (2006) Effects of ceramide on liquid-ordered domains investigated by simultaneous AFM and FCS. Biophys. J. 90, 4500–4508.

[14] Hannun, Y.A., Loomis, C.R., Merrill Jr., A.H. and Bell, R.M. (1986) Sphingosine inhibition of protein kinase C activity and of phorbol dibutyrate binding in vitro and in human platelets. J. Biol. Chem. 261, 12604–12609.

[15] Kolesnick, R.N. (1987) 1,2-Diacylglycerols but not phorbol esters stimulate sphingomyelin hydrolysis in GH3 pituitary cells. J. Biol. Chem. 262, 16759–16762.

[16] Taha, T.A., Mullen, T.D. and Obeid, L.M. (2006) A house divided: ceramide, sphingosine, and sphingosine-1-phosphate in programmed cell death. Biochim. Biophys. Acta 1758, 2027–2036.

[17] Huang, H.W., Goldberg, E.M. and Zidovetzki, R. (1996) Ceramide induces structural defects into phosphatidylcholine bilayers and activates phospholipase A2. Biochem. Biophys. Res. Commun. 220, 834–838.

[18] Kolesnick, R.N., Goñi, F.M. and Alonso, A. (2000) Compartmentalization of ceramide signaling: physical foundations and biological effects. J. Cell Physiol. 184, 285–300.

[19] Goñi, F.M. and Alonso, A. (2006) Biophysics of sphingolipids I. Membrane properties of sphingosine, ceramides and other simple sphingolipids. Biochim. Biophys. Acta 1758, 1902–1921.

[20] Megha and London, E. (2004) Ceramide selectively displaces cholesterol from ordered lipid domains (rafts): implications for lipid raft structure and function. J. Biol. Chem. 279, 9997–10004.

[21] Megha, Sawatzki, P., Kolter, T., Bittman, R. and London, E. (2007) Effect of ceramide N-acyl chain and polar headgroup structure on the properties of ordered lipid domains (lipid rafts). Biochim. Biophys. Acta 1768, 2205–2212.

[22] Alanko, S.M., Halling, K.K., Maunula, S., Slotte, J.P. and Ramstedt, B. (2005) Displacement of sterols from sterol/sphingomyelin domains in fluid bilayer membranes by competing molecules. Biochim. Biophys. Acta 1715, 111–121.

[23] Nybond, S., Björkqvist, Y.J., Ramstedt, B. and Slotte, J.P. (2005) Acyl chain length affects ceramide action on sterol/sphingomyelin-rich domains. Biochim. Biophys. Acta 1718, 61–66.

[24] Ridgway, N.D., Lagace, T.A., Cook, H.W. and Byers, D.M. (1998) Differential effects of sphingomyelin hydrolysis and cholesterol transport on oxysterol-binding protein phosphorylation and Golgi localization. J. Biol. Chem. 273, 31621–31628.

[25] Al-Makdissy, N., Younsi, M., Pierre, S., Ziegler, O. and Donner, M. (2003) Sphingomyelin/cholesterol ratio: an important determinant of glucose transport mediated by GLUT-1 in 3T3-L1 preadipocytes. Cell. Signal. 15, 1019–1030.

[26] Montes, L.R., Ibarguren, M., Goñi, F.M., Stonehouse, M., Vasil, M.L. and Alonso, A. (2007) Leakage-free membrane fusion induced by the hydrolytic activity of PlcHR(2), a novel phospholipase C/sphingomyelinase from *Pseudomonas aeruginosa*. Biochim. Biophys. Acta 1768, 2365–2672.

[27] Montes, L.R., Goñi, F.M., Johnston, N.C., Goldfine, H. and Alonso, A. (2004) Membrane fusion induced by the catalytic activity of a phospholipase C/sphingomyelinase from *Listeria monocytogenes*. Biochemistry 43, 3688–3695.

[28] Sot, J., Bagatolli, L.A., Goñi, F.M. and Alonso, A. (2006) Detergent-resistant, ceramide-enriched domains in sphingomyelin/ceramide bilayers. Biophys. J. 90, 903–914.

[29] Veiga, M.P., Arrondo, J.L., Goñi, F.M. and Alonso, A. (1999) Ceramides in phospholipid membranes: effects on bilayer stability and transition to nonlamellar phases. Biophys. J. 76, 342–350.

[30] López-Montero, I., Rodriguez, N., Cribier, S., Pohl, A., Vélez, M. and Devaux, P.F. (2005) Rapid transbilayer movement of ceramides in phospholipid vesicles and in human erythrocytes. J. Biol. Chem. 280, 25811–25819.

[31] Trajkovic, K., Hsu, C., Chiantia, S., Rajendran, L., Wenzel, D., Wieland, F., Schwille, P., Brügger, B. and Simons, M. (2008) Ceramide triggers budding of exosome vesicles into multivesicular endosomes. Science 319, 1244–1247.

[32] Basáñez, G., Ruiz-Argüello, M.B., Alonso, A., Goñi, F.M., Karlsson, G. and Edwards, K. (1997) Morphological changes induced by phospholipase C and by sphingomyelinase on large unilamellar vesicles: a cryo-transmission electron microscopy study of liposome fusion. Biophys. J. 72, 2630–2637.

[33] Sot, J., Aranda, F.J., Collado, M.I., Goñi, F.M. and Alonso, A. (2005) Different effects of long- and short-chain ceramides on the gel-fluid and lamellar-hexagonal transitions of phospholipids: a calorimetric, NMR, and X-ray diffraction study. Biophys. J. 88, 3368–3380.

[34] Tamba, Y., Ohba, S., Kubota, M., Yoshioka, H., Yoshioka, H. and Yamazaki, M. (2007) Single GUV method reveals interaction of tea catechin (−)-epigallocatechin gallate with lipid membranes. Biophys. J. 92, 3178–3194.

[35] Calhoun, W.I. and Shipley, G.G. (1979) Sphingomyelin–lecithin bilayers and their interaction with cholesterol. Biochemistry 18, 1717–1722.

[36] Ruiz-Argüello, M.B., Veiga, M.P., Arrondo, J.L., Goñi, F.M. and Alonso, A. (2002) Sphingomyelinase cleavage of sphingomyelin in pure and mixed lipid membranes. Influence of the physical state of the sphingolipid. Chem. Phys. Lipids 114, 11–20.

[37] Ladbrooke, B.D., Williams, R.M. and Chapman, D. (1968) Studies on lecithin–cholesterol–water interactions by differential scanning calorimetry and X-ray diffraction. Biochim. Biophys. Acta 150, 333–340.

[38] Mannock, D.A., Lewis, R.N. and McElhaney, R.N. (2006) Comparative calorimetric and spectroscopic studies of the effects of lanosterol and cholesterol on the thermotropic phase behavior

and organization of dipalmitoylphosphatidylcholine bilayer membranes. Biophys. J. 91, 3327–3340.
[39] Térová, B., Slotte, J.P. and Nyholm, T.K. (2004) Miscibility of acyl-chain defined phosphatidylcholines with *N*-palmitoyl sphingomyelin in bilayer membranes. Biochim. Biophys. Acta 1667, 182–189.
[40] Li, X.-M., Momsen, M.M., Smaby, J.M., Brockman, H.L. and Brown, R.E. (2001) Cholesterol decreases the interfacial elasticity and detergent solubility of sphingomyelins. Biochemistry 40, 5954–5963.
[41] Ira and Johnston, L.J. (2008) Sphingomyelinase generation of ceramide promotes clustering of nanoscale domains in supported bilayer membranes. Biochim. Biophys. Acta 1778, 185–197.
[42] Carrer, D.C. and Maggio, B. (2001) Transduction to self-assembly of molecular geometry and local interactions in mixtures of ceramides and ganglioside GM1. Biochim. Biophys. Acta 1514, 87–99.
[43] Taniguchi, Y., Ohba, T., Miyata, H. and Ohki, K. (2006) Rapid phase change of lipid microdomains in giant vesicles induced by conversion of sphingomyelin to ceramide. Biochim. Biophys. Acta 1758, 145–153.